Research Paper

Exosomes derived from BDNF-expressing 293T attenuate ischemic retinal injury in vitro and *in vivo*

Bojing Yan[1], Lixin Gao[1], Yingxiang Huang[1], Xiaolei Wang[1], Xuqiang Lang[1], Fancheng Yan[1], Bo Meng[1], Xiaowei Sun[2], Genlin Li[3], Yanling Wang[1]

[1]Department of Opthalmology, Beijing Friendship Hospital, Capital Medical University, Beijing 100050, China
[2]Department of Ophthalmology, Yantai Yuhuangding Hospital Affiliated to Medical College of Qingdao University, Qingdao 264000, China
[3]Beijing Tongren Eye Center, Beijing Tongren Hospital, Capital Medical University, Beijing Ophthalmology and Visual Sciences Key Lab, Beijing 100730, China

Correspondence to: Genlin Li, Yanling Wang; **email:** ligenlin2018@163.com, https://orcid.org/0000-0001-8926-3592; wangyanling999@vip.sina.com
Keywords: retinal ischemia, exosome, brain-derived neurotrophic factor, endocytosis, apoptosis
Received: March 11, 2020 **Accepted:** June 4, 2020 **Published:** November 29, 2020

ABSTRACT

Retinal ischemia emerges in many ocular diseases and is a leading cause of neuronal death and dysfunction, resulting in irreversible visual impairment. We previously reported that brain-derived neurotrophic factor (BDNF)-expressing human 293T cells could steadily express BDNF and play a protective role in ARPE-19 cells, a human retinal epithelial cell line. Thus, we hypothesized that exosomes might be essential in the interaction between BDNF-expressing 293T cells and recipient cells. The study investigated whether exosomes derived from BDNF-expressing 293T cells (293T-Exo) can be internalized by ischemic retinal cells and exert neuroprotective roles. The results demonstrated that 293T-Exo significantly attenuated the loss of cell proliferation and cell death in R28 cells in response to oxygen-glucose deprivation treatment. Mechanistic studies revealed that the endocytosis of 293T-Exo by R28 cells displayed dose- and temperature-dependent patterns and may be mediated by the caveolar endocytic pathway via the integrin receptor. In the retinal ischemia rat model, the administration of 293T-Exo into the vitreous humor of ischemic eyes reduced apoptosis in the retina. Furthermore, 293T-Exo was mainly taken up by retinal neurons and retinal ganglion cells. Together, the results demonstrated that 293T-Exo has a neuroprotective effect in retinal ischemia and has therapeutic potential for retinal disorders.

INTRODUCTION

Retinal ischemia-reperfusion (I/R) emerges in many ocular diseases and is a leading cause of neuronal death and dysfunction, resulting in irreversible visual impairment or blindness [1, 2]. Growing reports demonstrated that retinal ischemia is a primary contributor to the pathogenesis of multiple diseases, such as retinal vascular occlusions, diabetic retinopathy, central retinal vein occlusion, as well as age-associated macular degeneration [3]. However, an effective treatment for retinal ischemia is currently unknown, which leads to an urgent need to investigate the mechanisms and develop therapeutic strategies for retinal ischemia.

During ischemia, the deficiency of oxygen and other essential nutritional compounds generates reactive oxygen species due to subsequent restoration of oxygen supply, eventually leading to an inflammatory response and neurodegeneration [4, 5]. To study ischemia injury, retinal I/R animal models, including in vivo and ex vivo, have been established and widely employed to study the effect of I/R on neuronal

impairment in the retina [6]. In these animal models, intraocular pressure is dramatically raised above the systolic pressure for a specified time, followed by reperfusion treatment. Thus, several manifestations of I/R injury have been uncovered in such models, for example, the loss of retinal ganglion cells (RGCs), increased apoptosis in the inner retina, and decreased b waves [7].

Exosomes, 30-150 nm in diameter, are bi-lipid membrane extracellular vesicles (EVs) [8]. Due to their endocytic origin, EVs are categorized as exosomes, which contrasts with microvesicles that are produced from apoptotic bodies originated from fragments of dying cells or budding of the plasma membrane [9]. Exosomes are synthesized and released by various cell types and transport active biological molecules to regulate the physiological activities of recipient cells [10]. Thus, exosomes play an essential role in intercellular communication [11]. Over the past few decades, a growing number of studies suggest that the therapeutic effect of exosomes can facilitate repair and regeneration in multiple tissues, such as the heart [12], liver [13], and brain [14]. For retinal ischemia, bone marrow mesenchymal stem cells (MSCs)-derived exosomes can successfully transfer functional microRNAs into inner retinal layers and exert neuroprotective and axogenic roles in RGCs [15]. In addition, intravitreal administration of exosomes originated from human MSCs are well-tolerated and play a protective effect on retinal ischemia in a mouse model [16]. Together, exosome-mediated approaches are promising therapeutic strategies for retinal ischemia.

As the critical mediator in intercellular communication, the interaction between exosomes and recipients' cells is involved in a series of complicated processes [17]. In general, there are three main mechanisms involved in the exosome uptake, including 1) fusion with the recipient cells to transfer functional molecules, 2) binding to the surface receptor to initiate signaling cascades, and 3) internalization through phagocytosis, endocytosis, and macro-pinocytosis [18–20]. Also, several reports suggest that exosome-uptake proteins on the surface of exosomes and recipient cells also play an essential role in intercellular communication. For example, integrins are required for the exosome uptake in dendritic cells [19]. Clathrin and caveolin-associated pathways are two essential ways related to the endocytosis of exosomes [21]. So far, very few studies focus on the mechanism regarding how retinal cells uptake exosomes derived exogenous cells. Therefore, understanding the mechanism of exosome uptake would promote the development of more efficient delivery systems for disease treatment.

Brain-derived neurotrophic factor (BDNF), a member of the nerve growth factor gene family, is an essential multi-functional factor in various neuronal processes, including learning and memory, dendritic and synaptic plasticity, and axonal growth [22]. Beyond that, BDNF also has a broad effect on neuroprotection and regeneration in several neurodegenerative disorders, such as Alzheimer's, Parkinson's, and Huntington's disease [23, 24]. In addition, BDNF-transfected iris pigment epithelial (IPE) cells show a neuroprotective role against *N*-methyl-d-aspartate (NMDA)–associated neuroretinal cell death and phototoxic damage [25]. As previously reported [26], we constructed a eukaryotic BDNF-expressing plasmid from the human retina, and then subsequently used it to transfect human 293T cells. Our observations revealed that 293T cells transfected with the BDNF gene could steadily express BDNF mRNA and secrete the protein. Also, after coculturing with ARPE-19 cells, a human retinal epithelial cell line, increased level of BDNF is associated with higher viability and lower apoptosis in ARPE-19 cells, suggesting the potential neuroprotective role of BDNF in the retina.

Beyond that, several questions also emerged in this previous study: for example, what is the detailed mechanism underlying the role of BDNF-expressing cells and recipient cells and the role of BDNF in other retinal diseases? Given this, we hypothesized that exosomes might be an essential molecule-shuttle between BDNF-expressing 293T cells and recipient cells. We aimed to determine whether exosomes derived from BDNF-expressing 293T cells can be internalized by retinal cells and exert neuroprotective roles following ischemic injury and identify the related mechanism.

RESULTS

Characterization of 293T-Exo derived from BDNF-expressing 293T cells

We previously created human retina-derived BDNF plasmid construct in 293T cells. Next, we cocultured BDNF-expressing 293T cells with ARPE-19 in a Transwell chamber for 96 hours, and found that BDNF-engineered 293T cells exerted anti-apoptotic roles [26]. Given that, we assumed the potential role of exosomes in the interaction between BDNF-expressing 293T cells and recipient cells. Thus, we first isolated 293T-Exo from BDNF-expressing 293T cells. By NTA and TEM assays, the results showed that a majority of 293T-Exo (98.6%) were 144.2 nm in diameter and displayed a classic round-shape morphology (Figure 1A, 1B). In addition, the exosome surface markers CD9, CD63, CD81, and HSP70α were positively expressed in 293T-

Exo, but not in 293T-Exo-conditioned medium (Figure 1C). These results together demonstrated that we successfully isolated exosomes from BDNF-expressing 293T cells.

BDNF expression increased in 293T-Exo and 293T-Exo-treated R28 cells

Consistent with our previous results [26], mRNA and protein expressions of BDNF were increased in BDNF-expressing 293T cells compared with control untreated 293T cells (Figure 2A, 2B). Also, 293T-Exo expressed a higher level of BDNF than exosomes derived from control 293T cells (Figure 2A, 2B). After treating with 293T-Exo-conditioned medium or 293T-Exo, both mRNA and protein levels of BDNF were increased in R28 cells (Figure 2C, 2D), suggesting BDNF can be transferred from BDNF-expressing 293T cells to recipient R28 cells.

293T-Exo were endocytosed by R28 cells

As shown in Figure 3A, green fluorescence-labeled 293T-Exo was internalized by R28 cells. The overlapping of green color 293T-Exo with the red cytoskeleton demonstrated that 293T-Exo was uptaken in the cytoplasm. To determine the factors impacting the efficacy of endocytosis, we used different volumes of 293T-Exo (1-64 μl) to treat R28 cells, and the results suggested that the endocytosis reached a saturable status when the volume of 293T-Exo was 16 μl (Figure 3B). Also, we observed that higher temperatures (37° C) exerted a positive role in endocytosis, whereas low temperatures (4° C) inhibited the internalization of 293T-Exo (Figure 3C). Collectively, these results suggested that the endocytosis of 293T-Exo by R28 cells exhibited dose- and temperature-dependent patterns.

Integrin and caveolin-1 participated in the endocytosis of 293T-Exo

To determine more details of the endocytic process of 293T-Exo, we first used the specific ligands to test several critical endocytic receptors on the R28 plasma membrane, such as integrin and heparin sulfate proteoglycans (HSPGs) [27]. After pretreating R28 cells with RGD peptide, a specific ligand for integrin, we found that the endocytosis was significantly inhibited while no impact was observed on endocytosis when

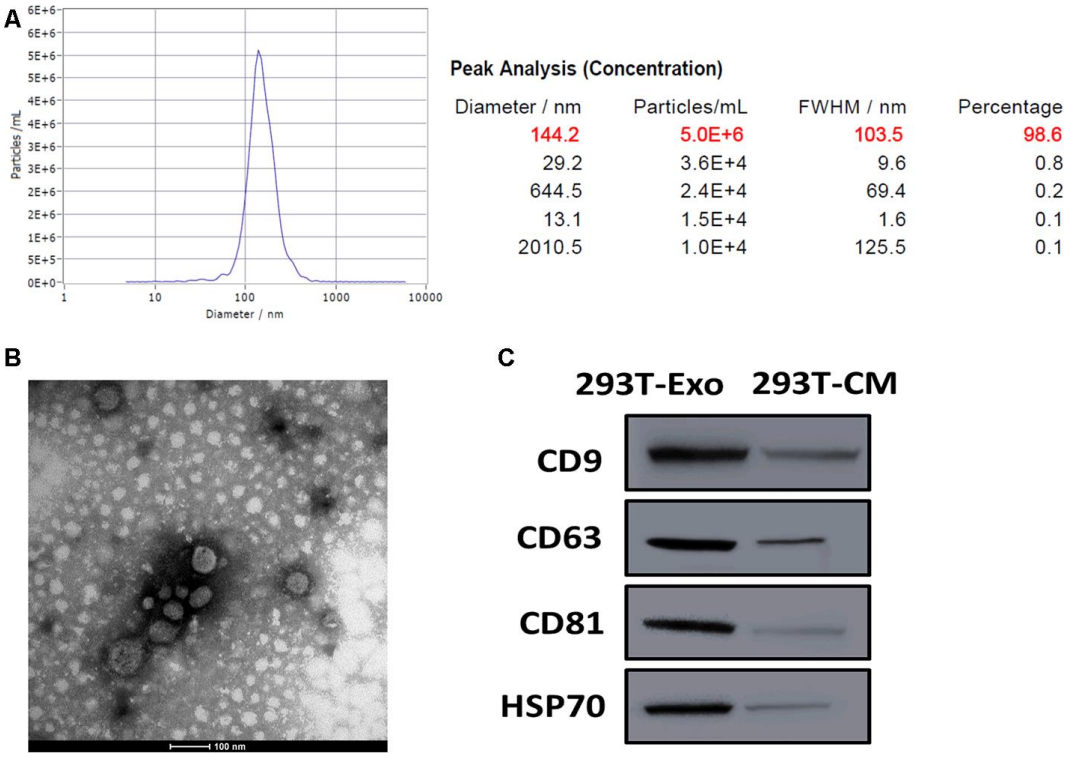

Figure 1. Characterization of 293T-Exo derived from BDNF-expressing 293T cells. (**A**) Diameter distribution of 293T-Exo determined by nanoparticle tracking analysis (NTA). (**B**) Representative image of 293T-Exo photographed by transmission electron microscopy (TEM). Scale bard = 100 nm. (**C**) Protein expressions of exosome surface markers, CD9, CD63, CD81, and HSP70α in 293T-Exo and 293T-Exo-conditioned medium (293T-CM), as measured using western blots.

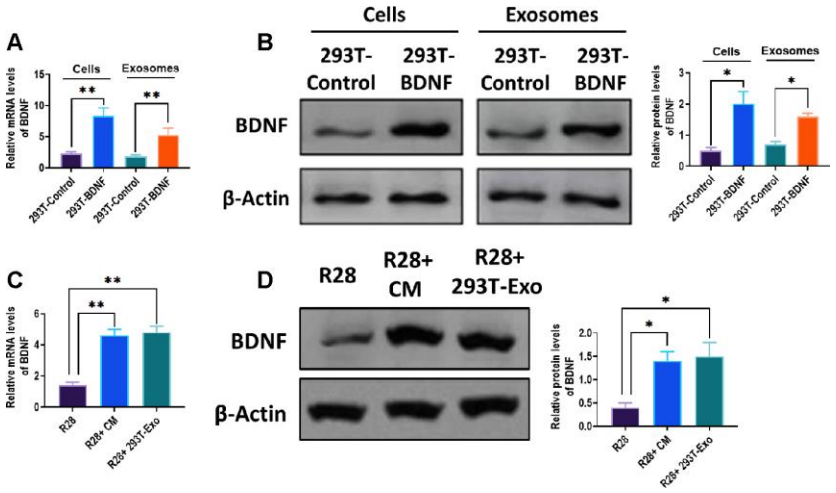

Figure 2. BDNF expression increased in 293T-Exo and 293T-Exo-treated R28 cells. mRNA (**A**) and protein (**B**) expressions of BDNF in control 293T cells, BDNF-expressing 293T cells, exosomes derived from control 293T cells, and BDNF-expressing 293T cells. mRNA (**C**) and protein (**D**) expressions in control R28 cells (R28), R28 cells treated with 293T-Exo-conditioned medium (R28+ CM), and R28 cells cocultured with 293T-Exo. Data are presented as mean ± SD. **P* < 0.05, ***P* < 0.01.

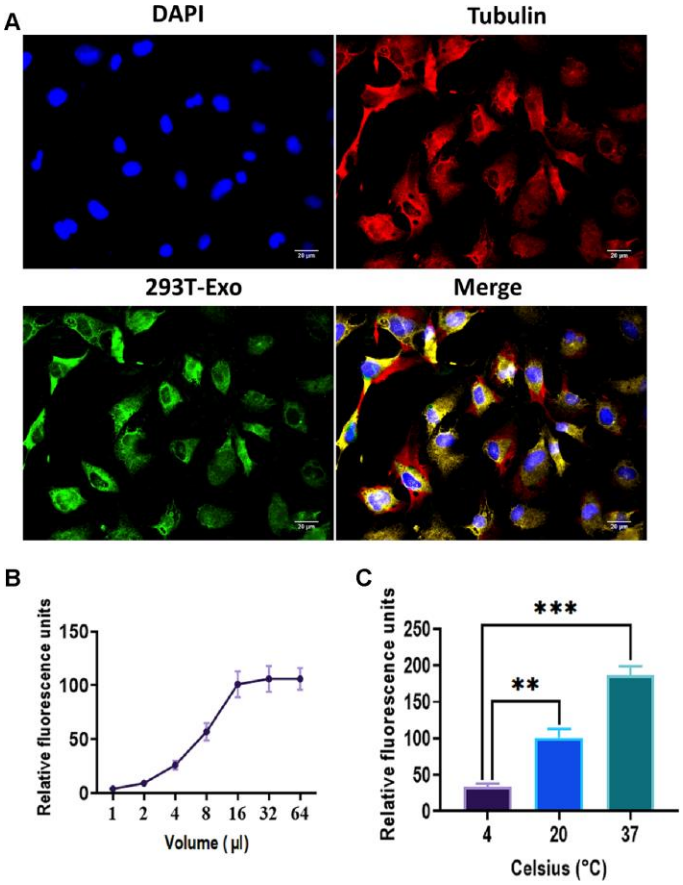

Figure 3. Endocytosis of 293T-Exo by R28 cells. (**A**) 293T-Exo uptake by R28 cells, as determined by the fluorescence assay. The nuclei were stained with DAPI (blue), the cytoskeleton was stained with tubulin (red), and 293T-Exo was stained with fluorescent-tag (green). Scale bar = 20 μm. (**B**) Efficacy of endocytosis of 293T-Exo by R28 cells displayed a dose-dependent pattern and saturable (more than 16 μl of 293T-Exo). (**C**) Efficacy of endocytosis of 293T-Exo by R28 cells displayed a temperature-dependent pattern. Data are presented as mean ± SD. ***P* < 0.01, ****P* < 0.001.

R28 cells were pretreated with heparin, a ligand for HSPGs (Figure 4A). In addition, a dose-dependent pattern was found in the effect of RGD on endocytosis of 293T-Exo, but not in heparin (Figure 4B, 4C). Clathrin and caveolin are two main pathways of endocytosis [28], therefore, we labeled those two markers with red fluorescence and found that green-293T-Exo colocalized with caveolin-1, but not clathrin (Figure 5). Furthermore, we applied MBCD to block the caveolin-1-associated endocytic process [29]. The results revealed that the endocytosis of 293T-Exo could be inhibited by MBCD in a dose-dependent pattern (Figure 6A, 6B). Taken together, these results demonstrated the involvement of integrin and caveolin-1 pathways in the endocytosis of 293T-Exo.

293T-Exo reduced R28 cell death in response to oxygen-glucose deprivation (OGD) *in vitro*

The OGD is widely applied to mimic ischemic conditions in vitro, promoting cell death [30]. To determine the role of 293T-Exo in OGD-treated R28 cells, we applied the EdU assay to measure the proliferation of R28 cells in the presence of OGD treatment. By flow cytometry analysis, we observed that both 293T-Exo and 293T-Exo-conditioned medium significantly increased the proliferative ability of R28 cells, compared with those treated with conditioned medium without 293T-Exo (Figure 7A). Meanwhile, the LDH assay showed that the reduction of cell death of OGD-treated R28 cells was accompanied by increasing doses of 293T-Exo (Figure 7B). These results together suggest a protective role of 293T-Exo for R28 cells in response to OGD.

Anti-apoptotic role of 293T-Exo *in vivo*

To determine whether 293T-Exo plays a protective role in retinal ischemia injury, we established a retinal ischemia rat model, and 293T-Exo was administered into the vitreous humor of ischemic eyes. Using the TUNEL assay, we observed that ischemia injury resulted in increased apoptosis in RGC, inner nuclear layers, and outer nuclear layers on the retinal tissue slides while the effect of ischemia injury was significantly attenuated by the administration of 293T-Exo (Figure 8A–8E).

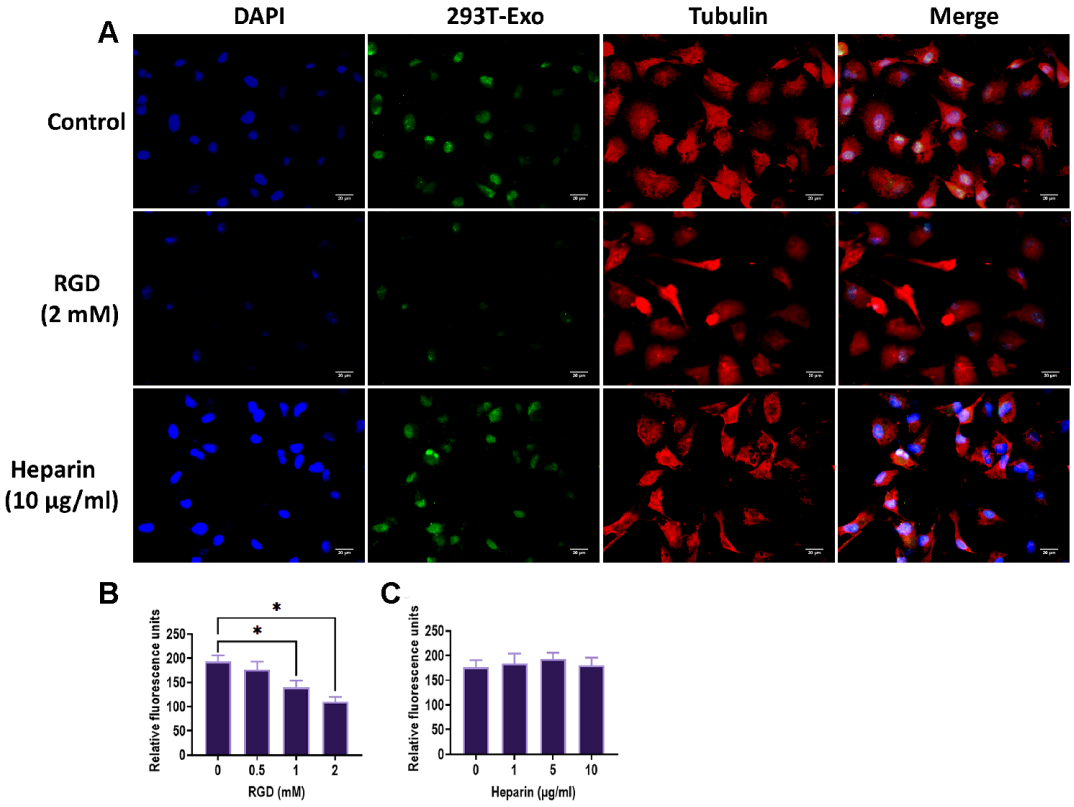

Figure 4. Integrins participated in the endocytosis of 293T-Exo by R28 cells. (**A**) Endocytosis was inhibited by pretreatment of RGD, but not by heparin. The nuclei were stained with DAPI (blue), the cytoskeleton was stained with tubulin (red), and 293T-Exo was stained with fluorescent-tag (green). Scale bar = 20 μm. (**B**) Efficacy of endocytosis of 293T-Exo by R28 cells was reversed due to increasing doses of RGD. (**C**) Efficacy of endocytosis of 293T-Exo by R28 cells was not affected by different doses of heparin. Data are presented as mean ± SD. *$P < 0.05$.

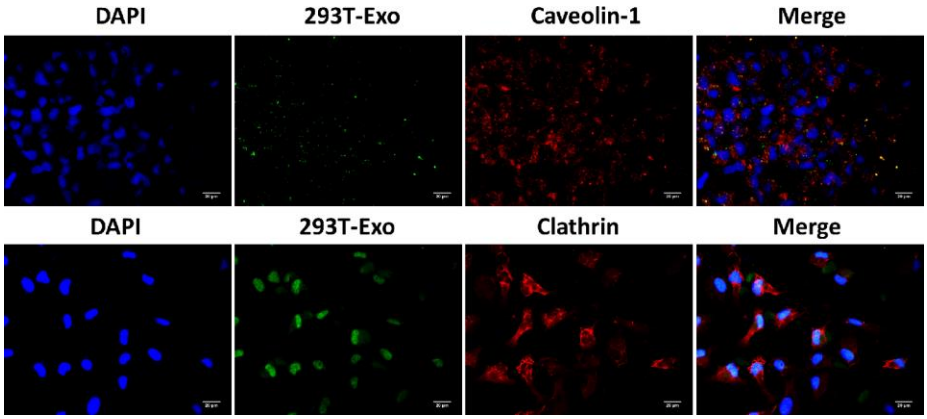

Figure 5. Caveolin-1 was involved in the endocytosis of 293T-Exo by R28 cells. The colocation of 293T-Exo with caveolin-1, but not clathrin, was observed using the fluorescence assay. The nuclei were stained with DAPI (blue), 293T-Exo was stained with fluorescent-tag (green), and the caveolin-1 or clathrin was stained with corresponding antibodies (red), respectively. Scale bar = 20 μm.

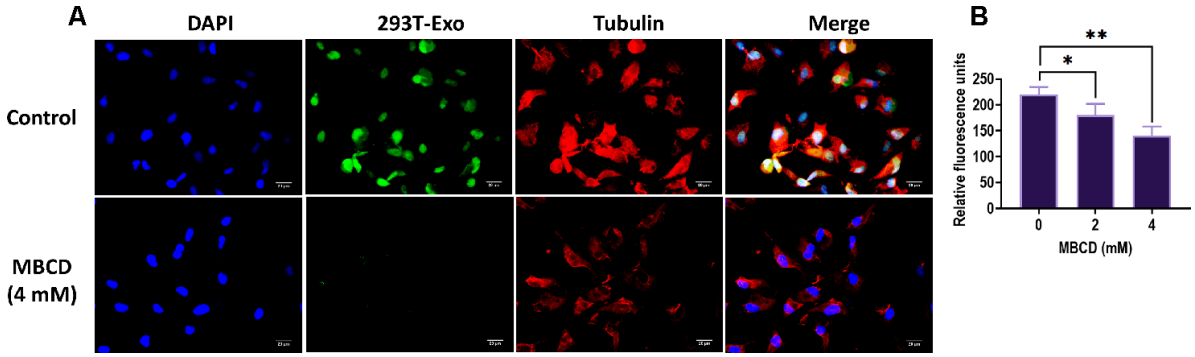

Figure 6. Caveolin-1-mediated endocytosis of 293T-Exo was inhibited by MBCD. (**A**) Pretreatment of MBCD in R28 cells inhibited the endocytosis of 293T-Exo, as determined by the fluorescence assay. The nuclei were stained with DAPI (blue), the cytoskeleton was stained with tubulin (red), and 293T-Exo was stained with fluorescent-tag (green). Scale bar = 20 μm. (**B**) Efficacy of endocytosis of 293T-Exo by R28 cells was reversed due to increasing doses of MBCD. Data are presented as mean ± SD. *$P < 0.05$, **$P < 0.01$.

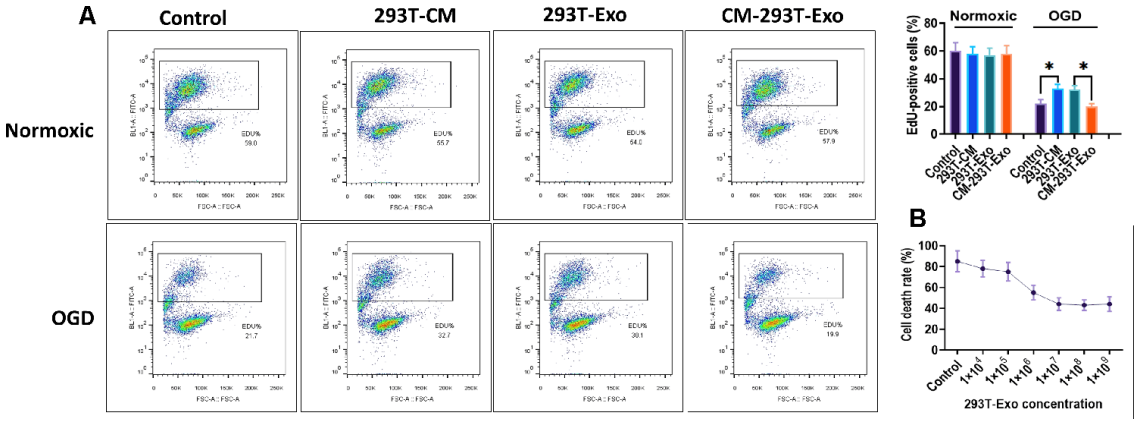

Figure 7. 293T-Exo inhibited OGD-induced cell death of R28 cells. (**A**) The percentage of EdU-positive in normoxic- or OGD-R28 cells with treatment of 293T-Exo, 293T-Exo-conditioned medium (293T-CM), and conditioned medium without 293T-Exo (CM-293T-Exo), as measured by flow cytometry. (**B**) Cell death rate was reduced by increasing concentration of 293T-Exo, as measured by the LDH assay. Data are presented as mean ± SD. *$P < 0.05$.

293T-Exo was endocytosed by the retinal neurons and RGCs

To determine the specific cell types that uptake 293T-Exo, the axonal or dendritic projections of retinal neurons were stained with red Beta III tubulin and the nuclei of RGCs were stained with magenta BRN3A. As shown in Figure 9, more colocalization of 293T-Exo with retinal neurons of RGCs was observed in retinal tissue slides in response to ischemia injury. These findings suggest that retinal neurons and RGCs are two main cell types that endocytose 293T-Exo.

DISCUSSION

It has been reported that ischemic injury activates several key protective pathways, including the neurotrophic family [31]. As an essential member of this family, BDNF exerts a significant neuroprotective role and facilitates neural repair and regeneration [32, 33]. Elevated expression of BDNF can protect retinal function and suppress apoptosis of retinal pigment epithelial cells and photoreceptors [34]. Given such an important role of BDNF, we previously created a human retina-derived BDNF-expressing construct in

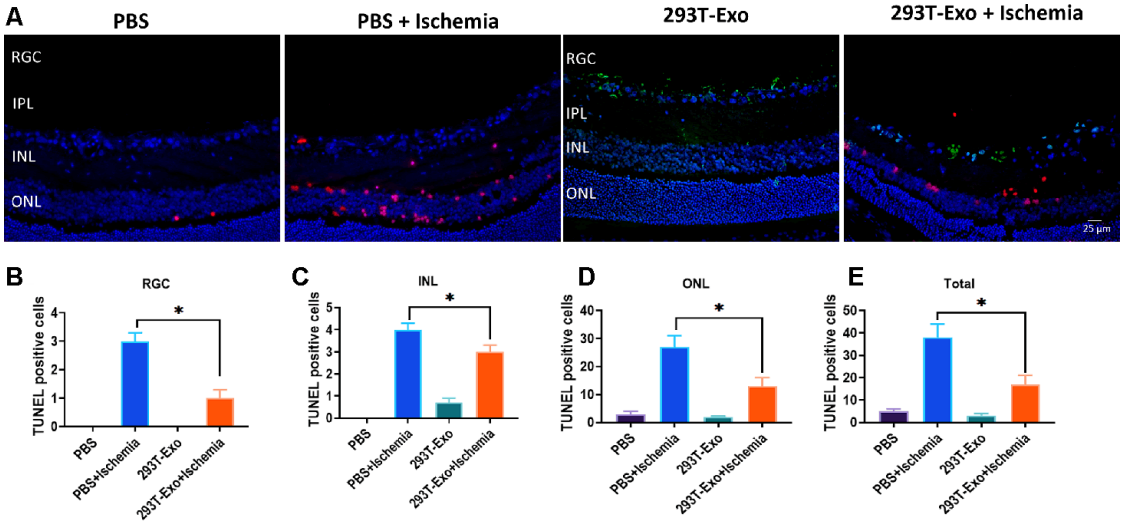

Figure 8. 293T-Exo inhibited OGD-induced apoptosis in the retinae in vivo. (**A**) 293T-Exo inhibited OGD-induced apoptosis in the retinae, as measured by the TUNEL fluorescence assay. The nuclei were stained with DAPI (blue), the TUNEL-positive cells were stained with TUNEL dye (red), and 293T-Exo was stained with fluorescent-tag (green). Scale bar = 25 μm. (**B**–**D**) Number of TUNEL-positive cells in different structural layers in the retinae in response to treatment of PBS, PBS+ Ischemia, 293T-Exo, and 293T-Exo+ Ischemia, respectively. (**E**) Total number of TUNEL-positive cells in the retinae in response to treatment of PBS, PBS+ Ischemia, 293T-Exo, and 293T-Exo+ Ischemia. RGC: retinal ganglion cell; IPL: inner plexiform layer; INL: inner nuclear layers; ONL: outer nuclear layers. Data are presented as mean ± SD. *$P < 0.05$.

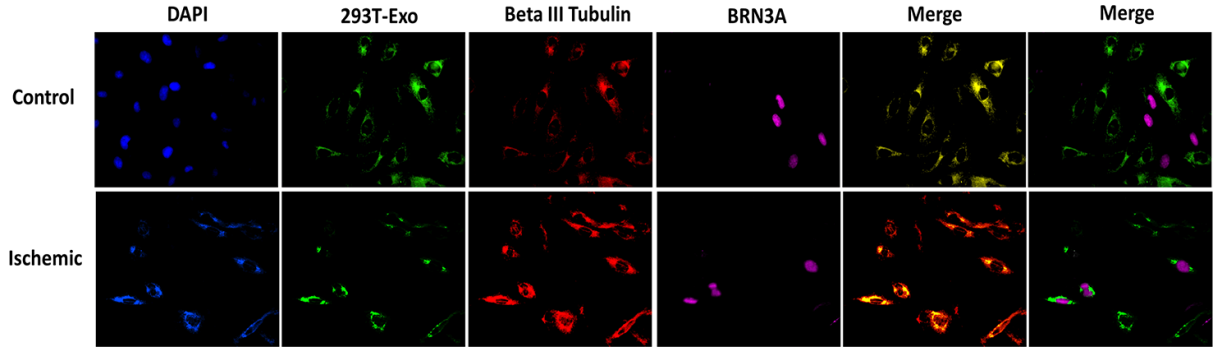

Figure 9. Endocytosis of 293T-Exo by retinal neurons and RGCs. Ischemia injury promoted endocytosis of 293T-Exo by retinal neurons and RGCs. The nuclei were stained with DAPI (blue), 293T-Exo was stained with fluorescent-tag (green), retinal neurons were stained with Beta III tubulin (red), and the nuclei of RGCs were stained with BRN3A (magenta). Scale bar = 25 μm.

293T cells from human retina and then investigated the effect of BDNF-expressing 293T cells in ARPE-19 cells, a retinal pigment epithelial cell line [26]. After coculturing BDNF- expressing 293T cells with ARPE-19 cells in a Transwell chamber, we found that ARPE-19 cells are more viable and display lower apoptotic levels. Given this, in the present study, we aimed to further investigate the mechanism underlying the neuroprotective role of BDNF-expressing 293T cells, specifically, to understand how BDNF-expressing 293T cells affect the recipient ARPE-19 cells.

Given the experimental design previously described [26], BDNF-expressing 293T cells cocultured with ARPE-19 cells in a Transwell chamber without direct contact, suggesting there may be a potential mediator in this interaction. In the past decade, exosomes have been demonstrated to be an essential mediator in intercellular communication and play an essential role in regulating physiological processes in recipient cells [10, 11]. Thus, we hypothesized that exosomes might be involved in the communication between BDNF-expressing 293T and ARPE-19 cells. To address this question, we successfully isolated exosomes from BDNF-expressing 293T cells and found that the expression of BDNF was significantly increased in 293T-Exo. Furthermore, these observations revealed that 293T-Exo may be internalized by R28 cells and result in an increased level of BDNF in R28 cells.

To further explore the detailed mechanism of this endocytic process, we performed experiments to demonstrate that the endocytosis of 293T-Exo by R28 cells displayed dose- and temperature-dependent patterns, indicating that the endocytosis may be mediated by endocytic receptors. To date, several distinct endocytic mechanisms have been reported to participate in the endocytosis of exosomes [18–20], of which, clathrin- and caveolare-mediated pathways have been demonstrated to be involved in the endocytosis of exosomes [27, 35]. For example, PC12 cell-derived exosomes carrying microRNA-21 are endocytosed by bone MSCs through a clathrin-mediated pathway [36]. Also, lipid raft-associated protein caveolin-1 can negatively regulate the internalization of exosomes derived from glioblastoma cells [28]. In the present study, colocalization of 293T-Exo with caveolin-1, but not clathrin, was found in R28 cells. Furthermore, our results showed that the RGD peptide, a specific ligand for integrin, significantly inhibited endocytosis. In contrast, heparin, a ligand for HSPGs, did not affect the endocytic process, suggesting that the endocytosis of 293T-Exo may be mediated by the caveolar endocytic pathway via a cell surface integrin receptor, a heterodimeric transmembrane receptor [37].

Next, regarding the function of 293T-Exo in R28 cells, we designed both in vitro and in vivo experiments to investigate the effect of 293T-Exo in retinal ischemia. Our results, in vitro, revealed that 293T-Exo inhibited cell death of R28 cells in response to OGD treatment. Consistently, 293T-Exo displayed a remarkable neuroprotective role in a retinal ischemia rat model through decreasing apoptosis in the retina. Furthermore, we also demonstrated that 293T-Exo was primarily internalized by retinal neurons and RGCs. Retinal ischemic injury is characterized by increased cell death, apoptosis, as well as neuroinflammatory responses, ultimately leading to RGC loss, blood-retinal barrier permeability, and blindness [38]. A growing number of studies report that the exosomes derived from MSCs can attenuate ischemia-induced injury in the retina. For example, exosomes derived bone MSCs can transfer functional microRNAs, rather than protein, into inner retinal layers and exert a significant therapeutic role in RGCs [15]. In addition, exosomes derived hypoxic human MSCs inhibit oxygen-induced retinopathy-induced retinal thinning and preserve retinal vascular flow, ameliorating the severity of retinal ischemia in a murine model [16]. As such, these findings together provide a new understanding of the mechanism underlying the effect of exosomes in ischemic retina.

Exosome-mediated therapies provide a cell-free alternative, relative to MSCs-based approaches. It has several notable advantages, such as easy operation (i.e., isolation, purification, storage, and delivery) and low risk (exosomes do not carry complications induced by transferring live cells into the vitreous). Meanwhile, there are still several challenges for exosome-based therapies. First, the safety and effectiveness of the dose of exosomes for each patient should be further investigated. Second, the timeframe of exosome-based therapies is essential for the clinical application. Third, the accuracy of delivering exosomes to the target tissue is a critical determinant for therapeutic purposes. Therefore, further studies should focus on addressing the above questions. Furthermore, it should be mentioned that we applied R28 retinal precursor cells, a transformed cell line [39], in vitro, which may not fully represent the function and structure of intact native retinal cells. Thus, it would be better to use native cells or tissues instead of transformed cells.

In conclusion, the results suggest that 293T-Exo is endocytosed by retinal cells through the caveolar endocytic pathway via the integrin receptor. In addition, 293T-Exo exerts a neuroprotective role in the ischemic retina, both in vitro and in vivo. The findings from the present study demonstrates a significant therapeutic potential of exosomes and provides an understanding of how to develop exosome-based therapies for retinal ischemia.

MATERIALS AND METHODS

Cell culture

As described in our previous study [26], human 293T cells were donated from the Functional Genomic Research Lab (Tsinghua University, China) and cultured in Dulbecco's Modified Eagle's Medium (DMEM; Cat#: A4192101; Thermo Fisher Scientific) supplemented with 10% heat-inactivated fetal bovine serum (FBS; Cat#: A3840001; Thermo Fisher Scientific) and 1% penicillin-streptomycin (Cat#: 15140122; Thermo Fisher Scientific) in a humidified incubator at 5% CO_2 and 37° C. Retinal cell line R28 (Cat#: EUR201; Kerafast) was cultured in DMEM supplemented with 10% fetal bovine serum (Cat#: A3160402; Thermo Fisher Scientific) and 100 μg/mL streptomycin (Cat#: 15140122; Thermo Fisher Scientific). The R28 cells were dissociated and used at a density of 1×10^6 cells/mL for all subsequent experiments.

Isolation exosomes derived from BDNF-expressing 293T cells

Construction of BDNF-expressing 293T cells was performed as previously described [26]. The protocol for isolation of 293T cell-derived exosomes (293T-Exo) was conducted as previously described [40–42]. Briefly, 293T cells were incubated in the FBS-free culture medium in 225-cm^2 flasks for 48 hours, and then the supernatants were collected. Cells, shedding vesicles, and cell fragments were removed from the supernatant through a series of centrifugation (300g*5 min, 3000 g*30 min, and 10,000 g*60 min). Total Exosome Isolation Reagent (Cat#: 4478359; Thermo Fisher Scientific) was used to isolate exosomes from cell culture medium according to the manufacturer's instruction. Afterward, exosomes were harvested from the pellets and resuspended in PBS. Then, 0.22-μm pore size polyvinylidene difluoride (PVDF) membrane filters (Cat#: GVWP04700; MilliporeSigma) were used to filter any remaining cells or debris. The concentration of exosome was quantified through the BCA Protein Quantification Assay (Cat#: ab 102536; Abcam) [43].

Transmission electron microscopy (TEM) and nanoparticle-tracking analysis (NTA)

The 293T-Exo sample preparation, TEM, and NTA were performed as previously described [42]. Morphology of 293T-Exo was determined through TEM assay with the transmission electron microscope (JEM-1010; JEOL Ltd.). The 293T-Exo size distribution was assessed using the NanoSight NS500 instrument and NTA (software version 2.3; Build 0033; Malvern Panlytical).

Real-time PCR

Total RNA was isolated from cells or exosomes using the Trizol Reagent kit (Cat#: 12183555; Thermo Fisher Scientific) according to the manufacturer's instruction. Reverse transcription was performed using the High-Capacity cDNA Reverse Transcription Kit (Cat#: 4368814; Thermo Fisher Scientific). The mRNA expressions were measured using the Fast SYBR™ Green Master Mix (Cat#: 4385612; Thermo Fisher Scientific) and the 7500 Fast Real-Time PCR System (Applied Biosystems). Real-time PCR data were analyzed using $2^{-\Delta\Delta Ct}$ method [44], and β-Actin was used as a reference control.

Western blots

The 293T-Exo (4 μg/ml), cells (1×10^6), or retinal tissues were lysed using T-PER™ Tissue Protein Extraction Reagent (Cat#: 78510; Thermo Fisher Scientific). Lysates were centrifuged and protein concentration was determined using the BCA Protein Quantification Assay (Cat#: ab 102536; Abcam). Ten μg protein was diluted with sodium dodecyl sulfate (SDS) sample buffer and loaded onto gels (4%–20%). Proteins were then electroblotted to polyvinylidene difluoride (PVDF) membranes (Cat#: 88518; Thermo Fisher Scientific). Protein-loaded membranes were incubated with primary antibodies overnight at 4° C on a shaker. The primary antibodies included: CD9 (1/500; Cat#: ab92726), CD63 (1/500; Cat#: ab134045), CD81 (1/500; Cat#: ab109201), HSP70 (1/1000; Cat#: ab5442), BDNF (1/500; Cat#: ab216443) and β-Actin (1/1000; Cat#: ab179467) (Abcam). Nonspecific binding was blocked with 5% non-fat dry milk in TBST. Protein band intensity was measured using Imagej software [45].

Fluorescence staining

The 293T-Exo was labeled with green fluorescent-tag using the ExoGlow-Protein Exosome/EV Protein Labeling Kit (Cat#: EXOGP300A-1-SBI; BioCat.) according to the manufacturer's instruction.

Establishment of retinal ischemia model in vitro

The R28 cells were subjected to the OGD assay to mimic ischemia injury [46]. Briefly, R28 cells (control) were cultured in normal medium to reach 80% confluence. For OGD treatment, R28 cells were cultured in glucose-free medium and then subjected to hypoxia condition (5% CO_2, 1% O_2) for 24 hours. Afterward, cells were supplied oxygen-enriched conditions (5% CO_2, 21% O_2) for 18 hours. Lactate dehydrogenase (LDH) assays (Cat#: ab102526; Abcam)

and ethynyl-deoxyuridine (EdU) assays (Cat#: ab219801; Abcam) were performed to measure cytotoxicity and proliferation according to the manufacturer's instruction.

Endocytosis assay

The R28 cells were plated in a 6-well plate and cocultured with 293T-Exo (50 μl) labeled with green fluorescent-tag or PBS for 1 hour at 37° C. Then, coverslips were washed with PBS and fixed with 4% neutral buffered formalin and stained with antibodies: clathrin (1/1000; Cat#: MA1-065), tubulin (1/1000; Cat#: MA1-118), and caveolin-1 (1/500; Cat#: PA1-064) (Thermo Fisher Scientific). Slides were photographed using fluorescence microscopy Observer.Z1 (Zeiss Axio). For the exosome dose-dependent experiments, R28 cells were incubated with different amounts of 293T-Exo (1, 2, 4, 8, 16, 32, and 64 μl) for 1 hour at 37° C. For the binding-blocking experiment, R28 cells (2×10^6) were pre-treated with Arginyl-glycyl-aspartic acid (RGD; 0, 0.5, 1 and 2 mM; Cat#: A9041-2MG; Sigma-Aldrich), heparin (0, 1, 5 and 10 μM; Cat#: 9041-08-1; Sigma-Aldrich), or MBCD (Methyl-β- cyclodextrin; 0, 2 and 4 mM; Cat#: C4555-1G; Sigma-Aldrich) at 4° C for 1 hour and then incubated with 50 μl 293T-Exo. Each well was washed with PBS three times and fixed with 4% neutral buffered formalin. The fluorescence was determined using fluorescence microscopy Observer.Z1 (Zeiss Axio).

Establishment of the retinal ischemia rat model

All animal-involved experimental procedures were approved by Beijing Friendship Hospital, Capital Medical University. Male Sprague Dawley rats (7-10 weeks old, 220-250 g, n=10) were used in this study. A retinal ischemia rat model was established as previously described [47]. Null-293T-Exo conditioned medium was prepared by isolating 293T-Exo from the medium. Normoxic Null-293T-Exo conditioned medium (5 μl), 293T-Exo (5 μl), or PBS (5 μl) were injected into the vitreous humor of both non-ischemic (left) and ischemic (right) eyes, 24 hours after retinal ischemia. The left eye was used as the control for each animal. Retinal tissues were collected at seven days post-injection.

TUNEL fluorescence assay

The TUNEL fluorescence assay was performed at 24 hours post-injection using the Cell Meter™ TUNEL Apoptosis Assay Kit (Cat#: 22844; Bioquest) according to the manufacturer's instruction. The TUNEL-positive cells were quantified using Imagej software [45].

Fluorescent assay for localization of 293T-Exo in rat retinal tissues

Control and ischemic male Sprague Dawley rats (7-10 weeks old, 220-250 g, n=10) were intravitreally injected with 293T-Exo labeled with green fluorescent-tag and anesthetized at seven days post-injection. The eyecup samples were prepared as previously described [46]. The primary antibodies were as follows: BRN3A (1/500; Cat#: ab81213), Beta III Tubulin (1/1000; Cat#: ab18207), and Iba1 (1/1000; Cat#: ab178846). Slides were photographed using the LSM 900 confocal microscope (ZEISS).

Statistical analysis

Data were presented as mean ± standard deviation (SD). Statistical analyses were performed using SPSS 13.0 software. At least three independent replicates were available in each experimental group. Statistical difference was determined by one-way ANOVA and t-test. $P < 0.05$ was considered statistically significant.

AUTHOR CONTRIBUTIONS

Bojing Yan, Lixin Gao and Yingxiang Huang performed the experiments and analyzed the data; Xiaolei Wang, Xuqiang Lang and Fancheng Yan performed the molecular investigations; Bo Meng and Xiaowei Sun collected the data, designed and coordinated the research; Genlin Li and Yanling Wang wrote the paper.

CONFLICTS OF INTEREST

These authors declare no conflicts of interest.

FUNDING

This project is funded by the National Natural Science Foundation of China (No. 81870686), National Natural Science Foundation of China (No. 81271046), and the Capital's Funds for Health Improvement and Research (No.2018-1-2021).

REFERENCES

1. Minhas G, Sharma J, Khan N. Cellular stress response and immune signaling in retinal ischemia-reperfusion injury. Front Immunol. 2016; 7:444. https://doi.org/10.3389/fimmu.2016.00444 PMID:27822213

2. Peng PH, Ko ML, Chen CF. Epigallocatechin-3-gallate reduces retinal ischemia/reperfusion injury by attenuating neuronal nitric oxide synthase expression

and activity. Exp Eye Res. 2008; 86:637–46. https://doi.org/10.1016/j.exer.2008.01.008 PMID:18289530

3. Osborne NN, Casson RJ, Wood JP, Chidlow G, Graham M, Melena J. Retinal ischemia: mechanisms of damage and potential therapeutic strategies. Prog Retin Eye Res. 2004; 23:91–147. https://doi.org/10.1016/j.preteyeres.2003.12.001 PMID:14766318

4. Korthuis RJ, Granger DN. Reactive oxygen metabolites, neutrophils, and the pathogenesis of ischemic-tissue/reperfusion. Clin Cardiol. 1993; 16:I19–26. https://doi.org/10.1002/clc.4960161307 PMID:8472394

5. McCord JM. Oxygen-derived free radicals in postischemic tissue injury. N Engl J Med. 1985; 312:159–63. https://doi.org/10.1056/NEJM198501173120305 PMID:2981404

6. Neufeld AH, Kawai Si, Das S, Vora S, Gachie E, Connor JR, Manning PT. Loss of retinal ganglion cells following retinal ischemia: the role of inducible nitric oxide synthase. Exp Eye Res. 2002; 75:521–28. https://doi.org/10.1006/exer.2002.2042 PMID:12457864

7. Renner M, Stute G, Alzureiqi M, Reinhard J, Wiemann S, Schmid H, Faissner A, Dick HB, Joachim SC. Optic nerve degeneration after retinal ischemia/reperfusion in a rodent model. Front Cell Neurosci. 2017; 11:254. https://doi.org/10.3389/fncel.2017.00254 PMID:28878627

8. Aguilera-Rojas M, Badewien-Rentzsch B, Plendl J, Kohn B, Einspanier R. Exploration of serum- and cell culture-derived exosomes from dogs. BMC Vet Res. 2018; 14:179. https://doi.org/10.1186/s12917-018-1509-x PMID:29884196

9. Merino-González C, Zuñiga FA, Escudero C, Ormazabal V, Reyes C, Nova-Lamperti E, Salomón C, Aguayo C. Mesenchymal stem cell-derived extracellular vesicles promote angiogenesis: potencial clinical application. Front Physiol. 2016; 7:24. https://doi.org/10.3389/fphys.2016.00024 PMID:26903875

10. Ng YH, Rome S, Jalabert A, Forterre A, Singh H, Hincks CL, Salamonsen LA. Endometrial exosomes/microvesicles in the uterine microenvironment: a new paradigm for embryo-endometrial cross talk at implantation. PLoS One. 2013; 8:e58502. https://doi.org/10.1371/journal.pone.0058502 PMID:23516492

11. Simons M, Raposo G. Exosomes—vesicular carriers for intercellular communication. Curr Opin Cell Biol. 2009; 21:575–81. https://doi.org/10.1016/j.ceb.2009.03.007 PMID:19442504

12. Lai RC, Arslan F, Lee MM, Sze NS, Choo A, Chen TS, Salto-Tellez M, Timmers L, Lee CN, El Oakley RM, Pasterkamp G, de Kleijn DP, Lim SK. Exosome secreted by MSC reduces myocardial ischemia/reperfusion injury. Stem Cell Res. 2010; 4:214–22. https://doi.org/10.1016/j.scr.2009.12.003 PMID:20138817

13. Tan CY, Lai RC, Wong W, Dan YY, Lim SK, Ho HK. Mesenchymal stem cell-derived exosomes promote hepatic regeneration in drug-induced liver injury models. Stem Cell Res Ther. 2014; 5:76. https://doi.org/10.1186/scrt465 PMID:24915963

14. Xiong Y, Mahmood A, Chopp M. Emerging potential of exosomes for treatment of traumatic brain injury. Neural Regen Res. 2017; 12:19–22. https://doi.org/10.4103/1673-5374.198966 PMID:28250732

15. Mead B, Tomarev S. Bone marrow-derived mesenchymal stem cells-derived exosomes promote survival of retinal ganglion cells through miRNA-dependent mechanisms. Stem Cells Transl Med. 2017; 6:1273–85. https://doi.org/10.1002/sctm.16-0428 PMID:28198592

16. Moisseiev E, Anderson JD, Oltjen S, Goswami M, Zawadzki RJ, Nolta JA, Park SS. Protective effect of intravitreal administration of exosomes derived from mesenchymal stem cells on retinal ischemia. Curr Eye Res. 2017; 42:1358–67. https://doi.org/10.1080/02713683.2017.1319491 PMID:28636406

17. Tian T, Zhu YL, Hu FH, Wang YY, Huang NP, Xiao ZD. Dynamics of exosome internalization and trafficking. J Cell Physiol. 2013; 228:1487–95. https://doi.org/10.1002/jcp.24304 PMID:23254476

18. Feng D, Zhao WL, Ye YY, Bai XC, Liu RQ, Chang LF, Zhou Q, Sui SF. Cellular internalization of exosomes occurs through phagocytosis. Traffic. 2010; 11:675–87. https://doi.org/10.1111/j.1600-0854.2010.01041.x PMID:20136776

19. Morelli AE, Larregina AT, Shufesky WJ, Sullivan ML, Stolz DB, Papworth GD, Zahorchak AF, Logar AJ, Wang Z, Watkins SC, Falo LD Jr, Thomson AW. Endocytosis, intracellular sorting, and processing of exosomes by dendritic cells. Blood. 2004; 104:3257–66. https://doi.org/10.1182/blood-2004-03-0824 PMID:15284116

20. McKelvey KJ, Powell KL, Ashton AW, Morris JM, McCracken SA. Exosomes: mechanisms of uptake. J

Circ Biomark. 2015; 4:7.
https://doi.org/10.5772/61186
PMID:28936243

21. Costa Verdera H, Gitz-Francois JJ, Schiffelers RM, Vader P. Cellular uptake of extracellular vesicles is mediated by clathrin-independent endocytosis and macropinocytosis. J Control Release. 2017; 266:100–08.
https://doi.org/10.1016/j.jconrel.2017.09.019
PMID:28919558

22. Linker RA, Lee DH, Demir S, Wiese S, Kruse N, Siglienti I, Gerhardt E, Neumann H, Sendtner M, Lühder F, Gold R. Functional role of brain-derived neurotrophic factor in neuroprotective autoimmunity: therapeutic implications in a model of multiple sclerosis. Brain. 2010; 133:2248–63.
https://doi.org/10.1093/brain/awq179
PMID:20826430

23. Zheng J, Sun J, Lu X, Zhao P, Li K, Li L. BDNF promotes the axonal regrowth after sciatic nerve crush through intrinsic neuronal capability upregulation and distal portion protection. Neurosci Lett. 2016; 621:1–8.
https://doi.org/10.1016/j.neulet.2016.04.006
PMID:27057731

24. Zuccato C, Cattaneo E. Brain-derived neurotrophic factor in neurodegenerative diseases. Nat Rev Neurol. 2009; 5:311–22.
https://doi.org/10.1038/nrneurol.2009.54
PMID:19498435

25. Kano T, Abe T, Tomita H, Sakata T, Ishiguro S, Tamai M. Protective effect against ischemia and light damage of iris pigment epithelial cells transfected with the BDNF gene. Invest Ophthalmol Vis Sci. 2002; 43:3744–53.
PMID:12454046

26. Yan BJ, Wu ZZ, Chong WH, Li GL. Construction of a plasmid for human brain-derived neurotrophic factor and its effect on retinal pigment epithelial cell viability. Neural Regen Res. 2016; 11:1981–89.
https://doi.org/10.4103/1673-5374.197142
PMID:28197196

27. Mulcahy LA, Pink RC, Carter DR. Routes and mechanisms of extracellular vesicle uptake. J Extracell Vesicles. 2014; 3.
https://doi.org/10.3402/jev.v3.24641
PMID:25143819

28. Svensson KJ, Christianson HC, Wittrup A, Bourseau-Guilmain E, Lindqvist E, Svensson LM, Mörgelin M, Belting M. Exosome uptake depends on ERK1/2-heat shock protein 27 signaling and lipid raft-mediated endocytosis negatively regulated by caveolin-1. J Biol Chem. 2013; 288:17713–24.
https://doi.org/10.1074/jbc.M112.445403
PMID:23653359

29. Mahammad S, Parmryd I. Cholesterol depletion using methyl-β-cyclodextrin. Methods Mol Biol. 2015; 1232:91–102.
https://doi.org/10.1007/978-1-4939-1752-5_8
PMID:25331130

30. Zhang F, Wang S, Signore AP, Chen J. Neuroprotective effects of leptin against ischemic injury induced by oxygen-glucose deprivation and transient cerebral ischemia. Stroke. 2007; 38:2329–36.
https://doi.org/10.1161/STROKEAHA.107.482786
PMID:17600230

31. Truettner J, Busto R, Zhao W, Ginsberg MD, Pérez-Pinzón MA. Effect of ischemic preconditioning on the expression of putative neuroprotective genes in the rat brain. Brain Res Mol Brain Res. 2002; 103:106–15.
https://doi.org/10.1016/s0169-328x(02)00191-2
PMID:12106696

32. Neumann JT, Thompson JW, Raval AP, Cohan CH, Koronowski KB, Perez-Pinzon MA. Increased BDNF protein expression after ischemic or PKC epsilon preconditioning promotes electrophysiologic changes that lead to neuroprotection. J Cereb Blood Flow Metab. 2015; 35:121–30.
https://doi.org/10.1038/jcbfm.2014.185
PMID:25370861

33. Zhang M, Mo X, Fang Y, Guo W, Wu J, Zhang S, Huang Q. Rescue of photoreceptors by BDNF gene transfer using in vivo electroporation in the RCS rat of retinitis pigmentosa. Curr Eye Res. 2009; 34:791–99.
https://doi.org/10.1080/02713680903086018
PMID:19839873

34. Azadi S, Johnson LE, Paquet-Durand F, Perez MT, Zhang Y, Ekström PA, van Veen T. CNTF+BDNF treatment and neuroprotective pathways in the rd1 mouse retina. Brain Res. 2007; 1129:116–29.
https://doi.org/10.1016/j.brainres.2006.10.031
PMID:17156753

35. Li C, Liu DR, Li GG, Wang HH, Li XW, Zhang W, Wu YL, Chen L. CD97 promotes gastric cancer cell proliferation and invasion through exosome-mediated MAPK signaling pathway. World J Gastroenterol. 2015; 21:6215–28.
https://doi.org/10.3748/wjg.v21.i20.6215
PMID:26034356

36. Tian T, Zhu YL, Zhou YY, Liang GF, Wang YY, Hu FH, Xiao ZD. Exosome uptake through clathrin-mediated endocytosis and macropinocytosis and mediating miR-21 delivery. J Biol Chem. 2014; 289:22258–67.
https://doi.org/10.1074/jbc.M114.588046
PMID:24951588

37. Lee HD, Kim YH, Kim DS. Exosomes derived from

human macrophages suppress endothelial cell migration by controlling integrin trafficking. Eur J Immunol. 2014; 44:1156–69.
https://doi.org/10.1002/eji.201343660
PMID:24338844

38. Mathew B, Poston JN, Dreixler JC, Torres L, Lopez J, Zelkha R, Balyasnikova I, Lesniak MS, Roth S. Bone-marrow mesenchymal stem-cell administration significantly improves outcome after retinal ischemia in rats. Graefes Arch Clin Exp Ophthalmol. 2017; 255:1581–1592.
https://doi.org/10.1007/s00417-017-3690-1
PMID:28523456

39. Seigel GM. Review: R28 retinal precursor cells: the first 20 years. Mol Vis. 2014; 20:301–06.
PMID:24644404

40. Hu Y, Yan C, Mu L, Huang K, Li X, Tao D, Wu Y, Qin J. Fibroblast-derived exosomes contribute to chemoresistance through priming cancer stem cells in colorectal cancer. PLoS One. 2015; 10:e0125625.
https://doi.org/10.1371/journal.pone.0125625
PMID:25938772

41. Chairoungdua A, Smith DL, Pochard P, Hull M, Caplan MJ. Exosome release of β-catenin: a novel mechanism that antagonizes Wnt signaling. J Cell Biol. 2010; 190:1079–91.
https://doi.org/10.1083/jcb.201002049
PMID:20837771

42. Li J, Chen X, Yi J, Liu Y, Li D, Wang J, Hou D, Jiang X, Zhang J, Wang J, Zen K, Yang F, Zhang CY, Zhang Y. Identification and characterization of 293T cell-derived exosomes by profiling the protein, mRNA and MicroRNA components. PLoS One. 2016; 11:e0163043.
https://doi.org/10.1371/journal.pone.0163043
PMID:27649079

43. Villarroya-Beltri C, Gutiérrez-Vázquez C, Sánchez-Madrid F, Mittelbrunn M. Analysis of microRNA and protein transfer by exosomes during an immune synapse. Methods Mol Biol. 2013; 1024:41–51.
https://doi.org/10.1007/978-1-62703-453-1_4
PMID:23719941

44. Schmittgen TD, Livak KJ. Analyzing real-time PCR data by the comparative C(T) method. Nat Protoc. 2008; 3:1101–08.
https://doi.org/10.1038/nprot.2008.73
PMID:18546601

45. Schneider CA, Rasband WS, Eliceiri KW. NIH image to ImageJ: 25 years of image analysis. Nat Methods. 2012; 9:671–75.
https://doi.org/10.1038/nmeth.2089
PMID:22930834

46. Mathew B, Ravindran S, Liu X, Torres L, Chennakesavalu M, Huang CC, Feng L, Zelka R, Lopez J, Sharma M, Roth S. Mesenchymal stem cell-derived extracellular vesicles and retinal ischemia-reperfusion. Biomaterials. 2019; 197:146–60.
https://doi.org/10.1016/j.biomaterials.2019.01.016
PMID:30654160

47. Rosenbaum DM, Degterev A, David J, Rosenbaum PS, Roth S, Grotta JC, Cuny GD, Yuan J, Savitz SI. Necroptosis, a novel form of caspase-independent cell death, contributes to neuronal damage in a retinal ischemia-reperfusion injury model. J Neurosci Res. 2010; 88:1569–76.
https://doi.org/10.1002/jnr.22314
PMID:20025059